Journal of Intelligent Manufacturing
https://doi.org/10.1007/s10845-020-01634-6

Control of deposition height in WAAM using visual inspection of previous and current layers

Jun Xiong[1] · **Yiyang Zhang**[1] · **Yupeng Pi**[1]

Received: 12 March 2020 / Accepted: 17 July 2020

Abstract
Wire plus arc additive manufacturing (WAAM) has been demonstrated to be a powerful technique to produce large-scale metal parts with low cost. However, techniques to achieve accurate geometry control and high process stability have not yet been perfectly developed. Although implementing vision sensing and closed-loop control can contribute to promoting the levels of process automation and stability, it is difficult to markedly improve the geometry precision of parts by only performing the current layer detection due to a large detection lag with vision-based sensors. To deal with this issue, this study proposes a novel strategy of introducing the previous layer information into the current deposition height to increase the response speed of the control system. The previous and current layer heights are monitored by a passive vision sensor. The height features are extracted by image processing algorithms mainly including edge detection, threshold division, and line fitting. Deviations in deposition height are automatically compensated via controlling the wire feed speed based on a PID controller. A helpful software interface is implemented in the Visual C++ environment to study the automatic detection and control system. In comparison to the closed-loop control using only the current layer detection, the deposition height of thin-walled parts can be excellently controlled by the proposed control system using the visual inspection of previous and current layers, significantly increasing the process stability and achieving accurate height control in WAAM.

Keywords Wire plus arc additive manufacturing · Automatic control · Visual sensing · Previous and current layers

Introduction

Metallic additive manufacturing (AM) is a novel technology that enables the production of near net shape metal parts layer upon layer, which allows increasing the design freedom, reducing the material wastage, and building complex assemblies (Demir 2018). In this field, wire plus arc additive manufacturing (WAAM) stands out among the metallic AM processes with great merits of higher deposition rates, lower equipment costs, and less contamination issues in comparison to laser or electron beam-based powder AM processes (Panchagnula and Simhambhatla 2018; Han et al. 2019). WAAM employs an arc as the power source to melt the filler wire, which is well suitable to fabricate large-size metal components and is gaining great popularity in the aerospace engineering filed, especially where the demand of building integral titanium or nickel alloys is increasing significantly (Van et al. 2020; Williams et al. 2016). Recently, a series of research efforts have been focused on WAAM, such as approaches for manufacturing complex-geometry parts (Panchagnula and Simhambhatla 2018; Li et al. 2020; Venturini et al. 2018), control of microstructure and mechanical properties (Ho et al. 2019), and thermal simulation of deposited parts (Cadiou et al. 2020).

In general, procedures in WAAM consist of establishment of a three-dimensional model, slicing the model into a series of layers, and stacking experiments. However, WAAM is sensitive to small variations in process parameters, and deposited layer geometries may fluctuate even with identical process variables. Moreover, WAAM operates in a layer by layer manner. Working conditions, parameter fluctuations, inter-layer temperatures, and states of previous layers can possess great actions on the current layer geometry, process stability, and dimensions of the final piece. Recently, some measures have been proposed to treat these issues, such as

✉ Jun Xiong
xiongjun@home.swjtu.edu.cn

[1] Key Laboratory of Advanced Technologies of Materials, Ministry of Education, School of Materials Science and Engineering, Southwest Jiaotong University, 111, Section 1 North Second Ring Road, Chengdu 610031, China

Published online: 24 July 2020

establishing mathematical models for layer geometry prediction (Xiong et al. 2014), control of inter-layer temperature using sensors (Chabot et al. 2019), implementing circulating cooling water in substrate (Yi et al. 2020) and imposing cooling gas on previous layers to alleviate heat accumulation (Wu et al. 2018), and integrating WAAM as an additive and milling as a subtractive technique to improve the surface quality (Zhang et al. 2019). Although aforementioned methods are able to improve the forming quality and precision of as-built parts, they cannot provide real-time monitoring and feedback information in WAAM.

To ensure the process stability and forming quality in WAAM, a highly promising strategy is to employ a sensing and control system to track and control deposited layer geometries. To our knowledge, the commonly used sensing techniques in arc-based processes are infrared, electric parameter, and vision detection. For instance, Yang et al. (2017) employed an infrared thermography to determine the temperatures of thin-walled parts deposited in gas metal arc (GMA) AM. However, the high device cost of the infrared system limits its wide application. Electric parameter sensing is also an effective detection technique in arc-based processes. In Bonaccorso et al. (2011), deposited heights in gas tungsten arc (GTA) AM were controlled using the arc voltage as the feedback information. Nevertheless, the arc voltage signal in arc-based processes fluctuates slightly and has a relatively low resolution with the arc length. Hence, this sensing method is suitable to circumstances without high requirements of control accuracy.

Vision sensing based on feedback measurements has been demonstrated to be a powerful tool to monitor the WAAM process (Radel et al. 2019). In general, it can be classified as passive or active sensing according to whether using an assistant light source (Xiong et al. 2016; Ding et al. 2016). As described in Comas et al. (2017), a passive imaging system was used for geometry measurement of the molten pool in plasma arc (PA) AM, and a novel camera calibration method was proposed. Doumanidis and Kwak (2002) designed a laser vision sensing system to detect the layer height and width in GMA AM, and a multi-variable controller in which the wire feed speed and travel speed were used as the controlling variables was developed for width and height control. In their work, the laser line was projected on the solidified metal which was 25.4 mm from the wire electrode, leading to a large delay of the detection system. Recent researches from Xiong and Zhang (2014) and Xiong et al. (2016) introduced passive vision sensors to detect the current layer width and deposition height in GMA AM, and closed-loop controllers were respectively designed to obtain consistent width or to compensate deposition height by tuning the travel speed.

GTA has fewer droplet transfer modes than GMA owing to the wire not being the consumable electrode (Marinelli et al. 2019). Hence, it is a more stable process and has a great potential to fabricate high-quality metals, receiving more attention in recent years. A previous study from Wang and Kovacevic (2001) employed a camera to monitor the arc length which was kept constant by controlling the torch height in GTA AM. It is evident that this control strategy cannot correspond to the concept of the AM process in which the deposited layer height should be equal to the given torch step height.

Although the application of feedback sensing and control can contribute to promoting the levels of process automation and stability, it is difficult to significantly improve the geometry precision of parts by only performing the current layer detection due to a large detection lag with the vision-based sensors explored in WAAM (Doumanidis and Kwak 2002; Xiong et al. 2016). In general, a control system with a large detection lag will produce serious overshoot, giving rise to an unsatisfied control precision for metal components. Considering that the previous layer information in front of the GTA torch can decrease the time lag of the detection system and enhance the prejudgment ability of the control system, this study proposes a novel strategy of introducing the previous layer information into the current deposition height to increase the response speed of the control system. A passive vision senor is designed to simultaneously monitor the previous and current layer heights in GTA AM. The height in the current layer is compensated by automatically tuning the wire feed speed. The proposed method will be particularly useful for decreasing the impact of the detection system's time lag and increasing the dimensional accuracy of fabricated parts. Section 2 presents the method including the system, image processing, and controller design, followed by Sect. 3 which depicts the experimental results and discussion. The last Sect. 4 ends the paper width some main conclusions.

Methods

System hardware

System overview

To investigate the process dynamics and control strategies in GTA AM, a simplified plant has been established in our lab with an industrial robot, a welding power supply, a wire feeder system, a passive vision sensor, a USB5831 data acquisition system, a modular software interface, and a control system, as shown in Fig. 1. The six-axis MOTOMAN-MH24 robot was responsible for the movement of the GTA torch. The welding power source was MagicWave 3000 Job G/F in which the current and wire feed speed can be adjusted separately. It should be noted that the KD 7000 wire feeder

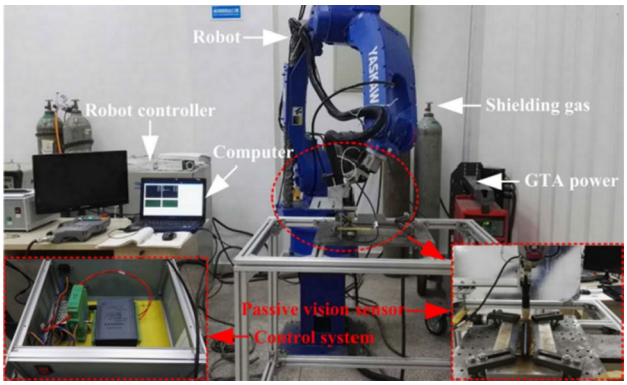

Fig. 1 Experimental layout in robotic GTA AM

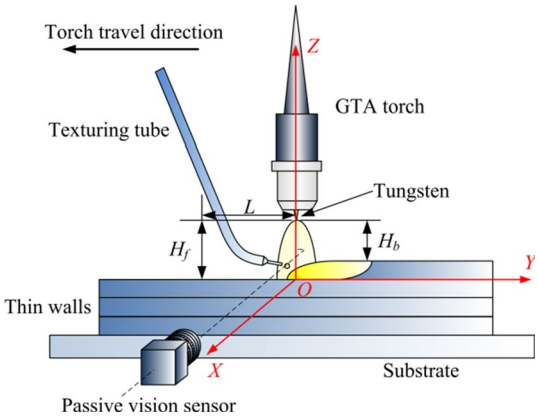

Fig. 2 Passive vision system design in robotic GTA AM

had a high response speed to the change in wire feed speed. As the core of the detection system, the passive vision sensor was applied to collect the previous and current layer heights. The modular software interface was designed to provide an operator all the visual and adjustment information from the system hardware.

The control system was designed to adjust the wire feed speed via external control signals. The USB5813 data acquisition card can output analog voltage ranging from 0 to 10 V to the Rob 5000 which was an external control interface developed by the Fronius company. To prevent signal interferences from the welding power source, an optoelectronic isolator was connected between the data acquisition card and the Rob 5000. In this circumstance, the wire feed speed of the GTA AM system can be controlled by the analog voltage signal from the data acquisition card.

Passive vision system design

Figure 2 presents a schematic diagram of the vision sensing system design in robotic GTA AM. The passive vision system, comprising a MER-125-30UM-L camera and a composite filter system (685 nm bandpass and 98% attenuator optics), was mounted on the GTA torch by a specially designed fixture. The relative position between the GTA torch and the sensor remained the same during fabrication. As illustrated in Fig. 2, the central axis of the camera is parallel to the X-axis, and the field of vision view was concentrated on a small area surrounding the tungsten tip, molten pool tail, and the previous layer in front of the arc. The vision images were collected using the camera with a resolution of 1292×964 and 8-bit gray scale at 30 fps refresh rate. To acquire the correlation between the image and the world coordinate system, a template with many square grids was applied to calibrate the sensor. The resolution in the image was calculated as 0.024 mm/pixel.

As shown in Fig. 2, the previous height H_f is the vertical distance between the tungsten tip and the previous layer, the current height H_b is the tungsten tip to the current layer surface distance, and the length L is the horizontal distance between the detection point and the tungsten tip. Ideally, during the deposition process, the amount of materials on each layer must be equal to the torch step height h imposed for the process. However, the deposition height is not always as prescribed due to unexpected perturbations to the operating conditions. Hence, the current height H_b is utilized to gather indirect information relating to the actual material deposited. To obtain a nearly constant H_b, the amount of deposited materials must be consistent with the torch step height h. It is worth noting that H_f is able to reflect the accumulated amount of materials deposited in previous layers. H_b in the current layer can be regarded as a disturbance action in the next layer. Essentially, H_f in the next layer equals the sum of the torch step height h and H_b in the current layer at the same point.

User interface

As presented in Fig. 3, a user interface is designed to provide information exchange between an operator and all the necessary information collected and calculated by the monitoring and control system. It mainly includes several modules, such as original image display, image processing, time series plot of wire feed speed and measuring heights, and setting given parameters. Visual C++ language was utilized to develop the modules, image processing, and control algorithms. As shown in Fig. 3, the image display including original and treated images is presented in the upper part, and the previous and current height information can be calculated by image processing. In the left bottom of the user interface, the time series plot of treated heights and wire feed speed are presented, and the data can be saved for offline analysis. In the right part, various buttons are designed for camera control, image conservation, offline image processing, and data playback. In the right bottom, a series of edit boxes are

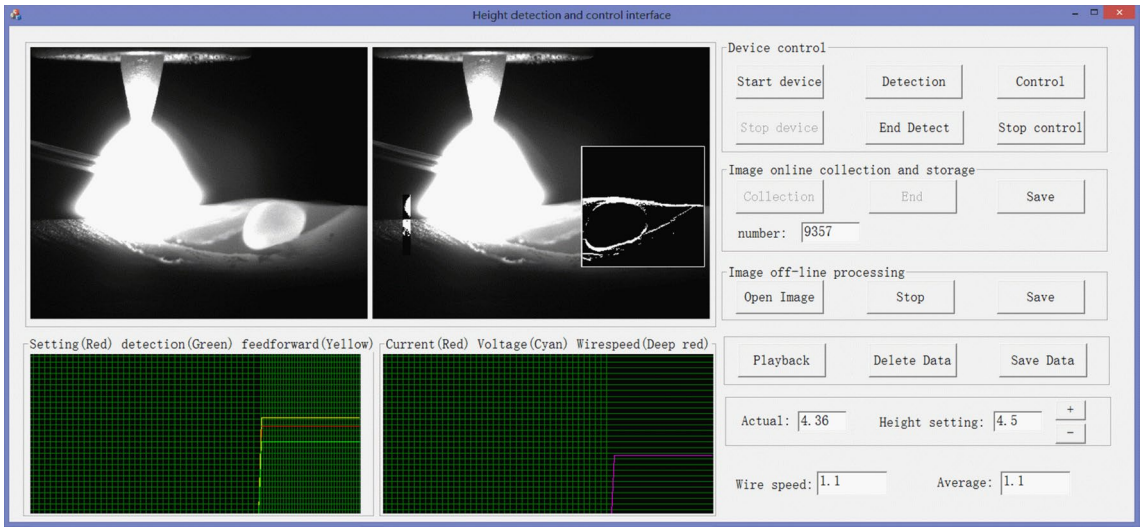

Fig. 3 User-friendly interface

produced for setting a given height and displaying measured heights as well as the wire feed speed.

Image processing for height tracking

The proposed image processing is applied to measure the previous height H_f and the current height H_b. Considering that the position of the tungsten tip in captured images is fixed, the premise of calculating H_f and H_b is to extract the previous and the current layer surfaces using image processing procedures.

This section provides a case study to detect the height information. One assumption is made that the image collection from one frame to another is smooth. In arc-based processes, this assumption is effective because the camera with a 30 fps sampling frequency is enough to observe the molten pool in which the change will hardly be abrupt (Comas et al. 2017).

The flow chart of image processing procedures for height detection is given in Fig. 4. The steps to detect the height information are detailed as follows.

1. *Image analysis and apply two windows* To know the best detection position, the captured image should be analyzed. The detection position on the previous layer needs to be set appropriately, which can not only be free from disturbances from the strong arc lights but can also make use of illumination from the arc. The detection point on the current layer should be located on the molten pool tail. The reason is that there is a strong oscillation on the molten pool surface due to the arc force's effect, and detecting the solidified layer increases the time lag of the sensor system. Based on the detection locations of previous and current layers, two small windows are applied to the interesting areas, allowing lowering the calculation cost of the image.

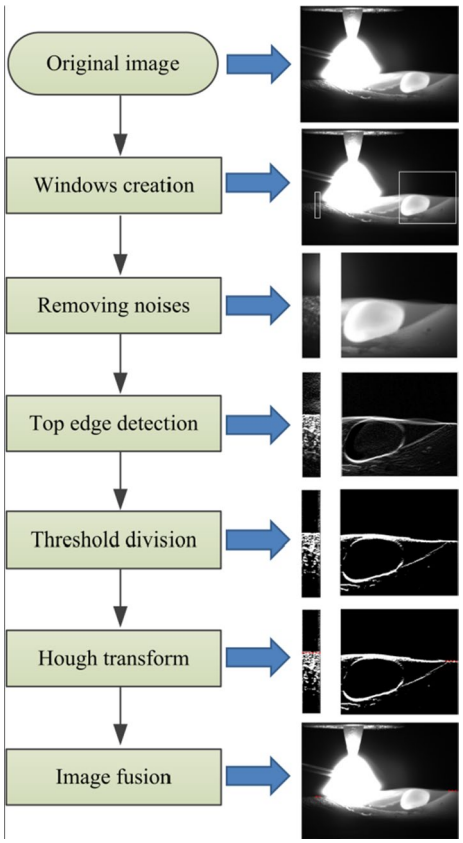

Fig. 4 Flow chart of image processing procedures for deposition height measurements

2. *Removing noise* In general, the quality of captured images may be influenced by a series of factors, such as fumes, inclusions, image distortion, and photoelectric signal transmission. To remove noise in the image resulting from image signal transmission and scattered stray lights from the arc lights, a Gaussian filter (Baxes 1994), in which a large weight coefficient is applied in the center and gradually decreased weights are employed away from the center, is used to smooth the image in both small windows. The Gaussian filter is given as

$$f(x,y) = \frac{1}{2\pi\sigma^2}\exp(-(x^2+y^2)/2\sigma^2) \tag{1}$$

where σ is the Gaussian radius, x and y are column and row coordinates, respectively.

3. Top edges detection: After removing noises, a Sobel edge detector capable of detecting abrupt changes of pixel intensity is utilized to identify boundaries between the deposited layers and the background (Marr and Hildreth 1980), which can be expressed as

$$f(x,y) = |\Delta f_x| + |\Delta f_y| \tag{2}$$

where Δf_x and Δf_y are the second-order differences of the gray value in the x-axis and y-axis, respectively.

4. Threshold segmentation: To further strengthen the edge features determined by the Sobel edge detector, the Otsu's thresholding method (Otsu 1979) is implemented to determine an optimal threshold in each small window, which can help to determine the strongest edge.

5. Edge line detection: After applying the threshold segmentation, the edge points on the top surface of the current and previous layers can be measured by scanning each column from the top of both small windows, respectively. However, the enhanced edges exhibit a series of discrete points, the aim of this step is to remove noises which may introduce false edges. A Hough transformation algorithm is applied to fit these discrete points, which is expressed as

$$a\cos\theta + b\sin\theta = \rho \tag{3}$$

where a and b are coordinate axes in the rectangular coordinate, θ and ρ are coordinate axes in the polar coordinate.

Figure 5 gives the results of height detections during deposition based on the proposed image processing method. The continuous detection data using the vision system is plotted by the solid curves. To validate the accuracy of the detection values, the deposition heights in the sampled images were manually measured, and the results are plotted by dotted curves in Fig. 5. It is seen that the height obtained from visual detection is in good agreement with the measured results. The average errors between the detected and manually measured values are less than 0.04 mm.

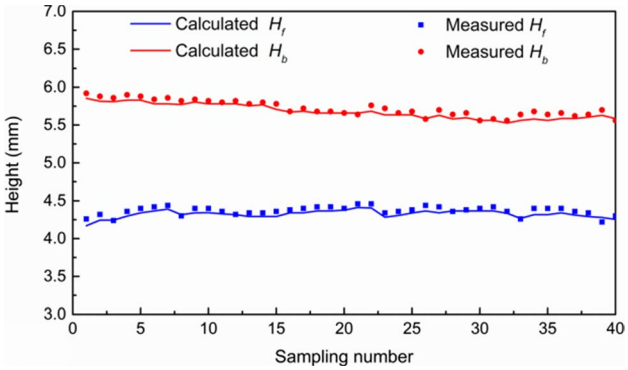

Fig. 5 Continuous previous and current height detection

Control strategy

GTA AM is a multi-layer deposition process, which is especially sensitive to process variables and heat accumulation during the fabrication process, leading to poor process stability and even process termination. Hence, the deposition height must be controlled to keep consistent with the slicing process. A promising approach is to design a closed-loop controller to compensate the deposition height by adjusting the wire feed speed in real time. The reason for choosing the wire feed speed as the controlling variable is that it has the strongest effect on height geometry in comparison to the arc current which can also influence the uniform energy rate (Bonaccorso et al. 2011). Additionally, the travel speed is not suitable to be online adjusted in robotic motion. Although regulating the wire feed speed during fabrication can slightly influence the layer width, the inconsistent widths of thin-walled parts can be treated during the subsequent fine machining process.

PID controller, which is extensively applied in the industrial control field due to its strong reliability and robustness, is utilized for automatic height control in GTA AM. In general, the PID algorithm in the analog control system is given as

$$u(t) = K_p E(t) + \frac{K_p}{T_i}\int_0^t E(t)dt + K_p T_d \frac{dE(t)}{dt} \tag{4}$$

where $u(t)$ is the controlling variable, K_p, T_i, and T_d are proportional, integral time, and derivative time coefficients, respectively, t is the time, and $E(t)$ is the control deviation between the measured results $m(t)$ and given value $r(t)$, which can be written as

$$E(t) = r(t) - m(t) \tag{5}$$

In the computer-integrated control system, the controlling variable is suitable to be given as discrete and incremental form at time t

$$\Delta u(t) = K_p P(t) + \beta K_i I(t) + K_d D(t) \tag{6}$$

where $\Delta u(t)$ is the increment of the wire feed speed, $K_i = K_p/T_i$, and $K_d = K_p T_D$, β is an integral-separation coefficient which is determined based on the threshold of $E(t)$. $P(t)$, $I(t)$, and $D(t)$ are given by:

$$\begin{aligned} P(t) &= E(t) - E(t-1) \\ I(t) &= E(t) \\ D(t) &= E(t) - 2E(t-1) + E(t-2) \end{aligned} \tag{7}$$

To decrease the time lag in the conventional feedback detection system, the previous height H_f capable of reflecting accumulated deviations between the deposited and ideal height of previous layers is introduced in the feedback control system. The previous step number d can be calculated as

$$d = [L/V_s T] \tag{8}$$

where L is the horizontal distance between the detection point and the tungsten tip, as presented in Fig. 2, V_s is the travel speed, and T is the sampling period of the detection system.

In this research, the controlled variable is the current height H_b. At time t, the current detection deviation $E_1(t)$ and previous detection deviation $E_2(t–d)$ can be respectively written as

$$E_1(t) = S_1 - H_b(t) \tag{9}$$

$$E_2(t-d) = S_2 - h - H_f(t-d) \tag{10}$$

where S_1 is the given current height, S_2 is the given previous height, $H_b(t)$ is the detected current height at time t, h is the slicing height regarded as the GTA torch step height when a layer is fabricated, and $H_f(t–d)$ is the previous detection height at time $(t–d)$.

By introducing the previous height at time $(t–d)$ in the current height at time t, the control deviation $E(t)$ of the detection system can be expressed as

$$E(t) = E_1(t) + E_2(t-d) \tag{11}$$

Results and discussion

Thin-walled parts were fabricated to validate the effectiveness of the closed-loop control system. The metal wire was ER50-6 with 1.2 mm diameter and the substrate was low-carbon steel Q235B. Table 1 lists the basic operating parameters used in GTA AM. The initial tungsten to substrate distance was set at 5.5 mm. During the fabrication process, as one layer was completed, the arc was turned off and the GTA torch was raised by a slicing height of 1.0 mm. Before starting a new layer, there existed an inter-layer idle time of 60 s to prevent the molten pool overflow induced by a high inter-layer temperature (Xiong et al. 2018). It is noted that the travel directions between adjacent layers were opposite, which was realized by modifying the robot pose.

Table 1 Operating parameters in GTA AM

Process parameters	Value
Arc current	150 A DC mode
Torch travel speed	4 mm/s
Wire feed mode	Front feeding
Shielding gas	99.99% Ar with 15 L/min
Size of substrate	150 mm × 80 mm × 4 mm
Initial wire feed speed	1.1 m/min

Two kinds of tests were performed, i.e., closed-loop control using current height detection and closed-loop control based on previous and current height detections. The data sampling period of the detection system is 0.25 s, and the control period of the control system is 0.5 s. In closed-loop control test using current height detection, only the current detection deviation $E_1(t)$ is considered. In closed-loop control based on previous and current height detections, the control deviation $E(t)$ is described in Eq. (11).

Closed-loop control using current height detection

In the closed-loop control test using current height detection, a 25-layered wall was fabricated by applying the PID controller to adjust the wire feed speed. Figure 6 presents the detected current heights H_b and adjusted wire feed speeds in various layers. It is seen that the detected current height of different layers can vacillate around the given current height, which is beneficial to increasing the process stability. However, the maximum deviation and fluctuation degree of the detected H_b increase along with the deposition height. The root mean square errors of the detected H_b curves in Fig. 6a–d are 0.118, 0.151, 0.3, and 0.3, respectively. The fluctuation degree of detected H_b can be used as a metric to quantify the total height evenness of the deposited wall. As shown in Fig. 6e, the flatness on the top surface of the 25-layered thin wall seems poor.

Closed-loop control using previous and current height detection

To further improve the process stability in GTA AM, the accumulated deviation of previously deposited layers is

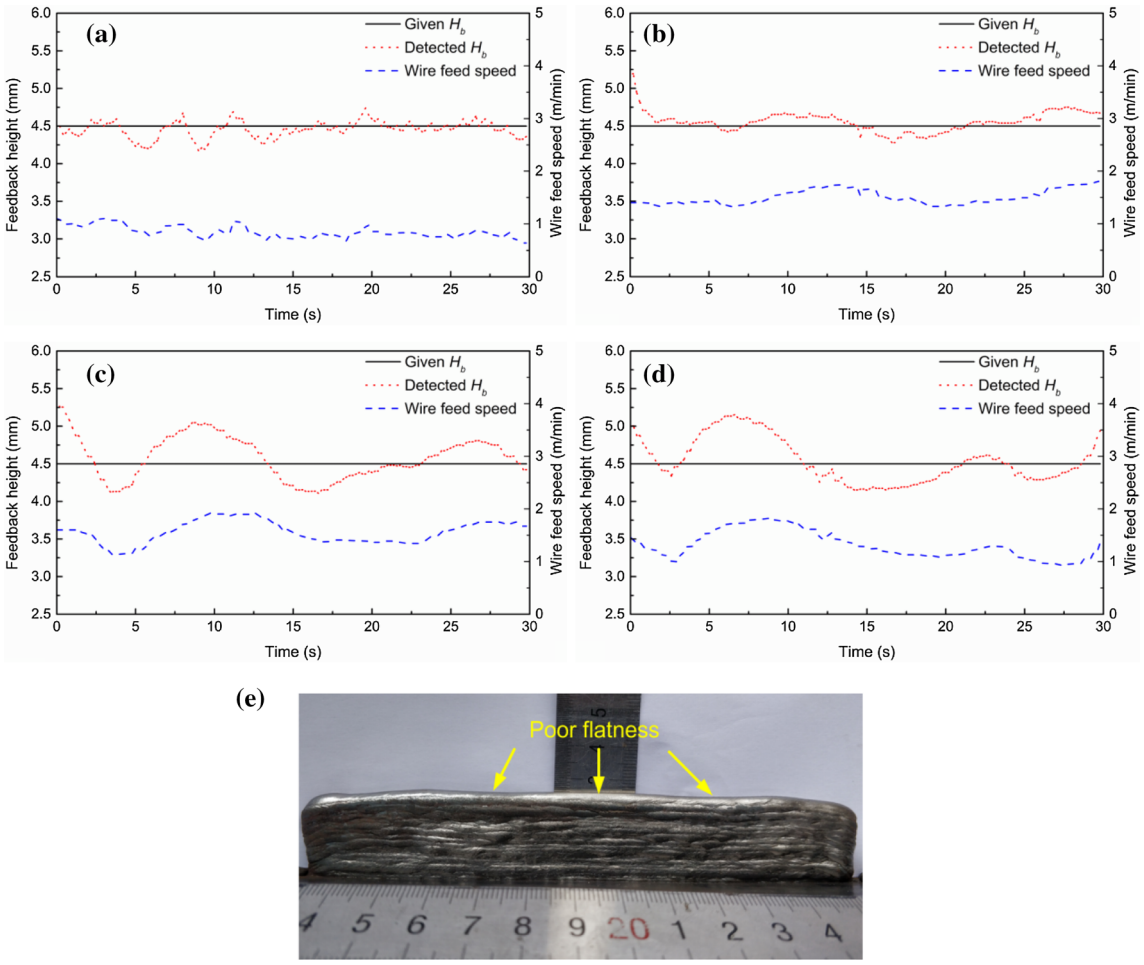

Fig. 6 Closed-loop control test based on current height detection. **a** Detected H_b and wire feed speed in 2nd layer. **b** Detected H_b and wire feed speed in 6th layer. **c** Detected H_b and wire feed speed in 16th layer. **d** Detected H_b and wire feed speed in 23th layer. **e** Macroscopic morphology of the 25-layered wall

added to the current height detection deviation, as depicted in Eq. (11). By introducing the previous height deviation in front of the arc, the wire feed speed in the control system can be adjusted in advance. Figure 7 displays the detected previous and current heights as well as the adjusted wire feed speed in various layers. As seen in Fig. 7, the detected H_f can reflect the height uniformity of previously deposited layers. In comparison to Fig. 6, the detected H_b fluctuates slightly around the given H_b. The root mean square errors of the detected H_b curves in Fig. 7a–d are 0.214, 0.202, 0.197, and 0.247, respectively. The maximum error of the current heights in Fig. 7 is less than 0.5 mm, and root mean square error is less than 0.25. Figure 7e shows the macroscopic morphology of the 25-layered wall deposited by applying the PID controller based on the visual detection of the previous and current heights. It appears that the flatness of the top layer surface is better than that presented in Fig. 6e. This is confirmed by considering the root mean square error which is consistently lower than that in the pure current height detection case, i.e., 0.247 compared to 0.3 at the 23rd layer.

Control mechanism using previous and current height detection

The mechanism for closed-loop control based on the previous and current heights needs to be discussed. By applying the closed-loop controller based on only the current height detection, the deposited *Hb* curve exhibits fluctuations around the given value due to characteristics of feedback control. However, time lag is a main difficulty for the traditional feedback control. It is shown in Fig. 2 that the detection position of the current height is set at a large horizontal distance from the tungsten tip due to a long molten pool length resulted from the heat accumulation and poor heat conduction condition. The detected information at the molten pool tail is outdated, leading to a time lag of the detection system and a large overshoot of the feedback

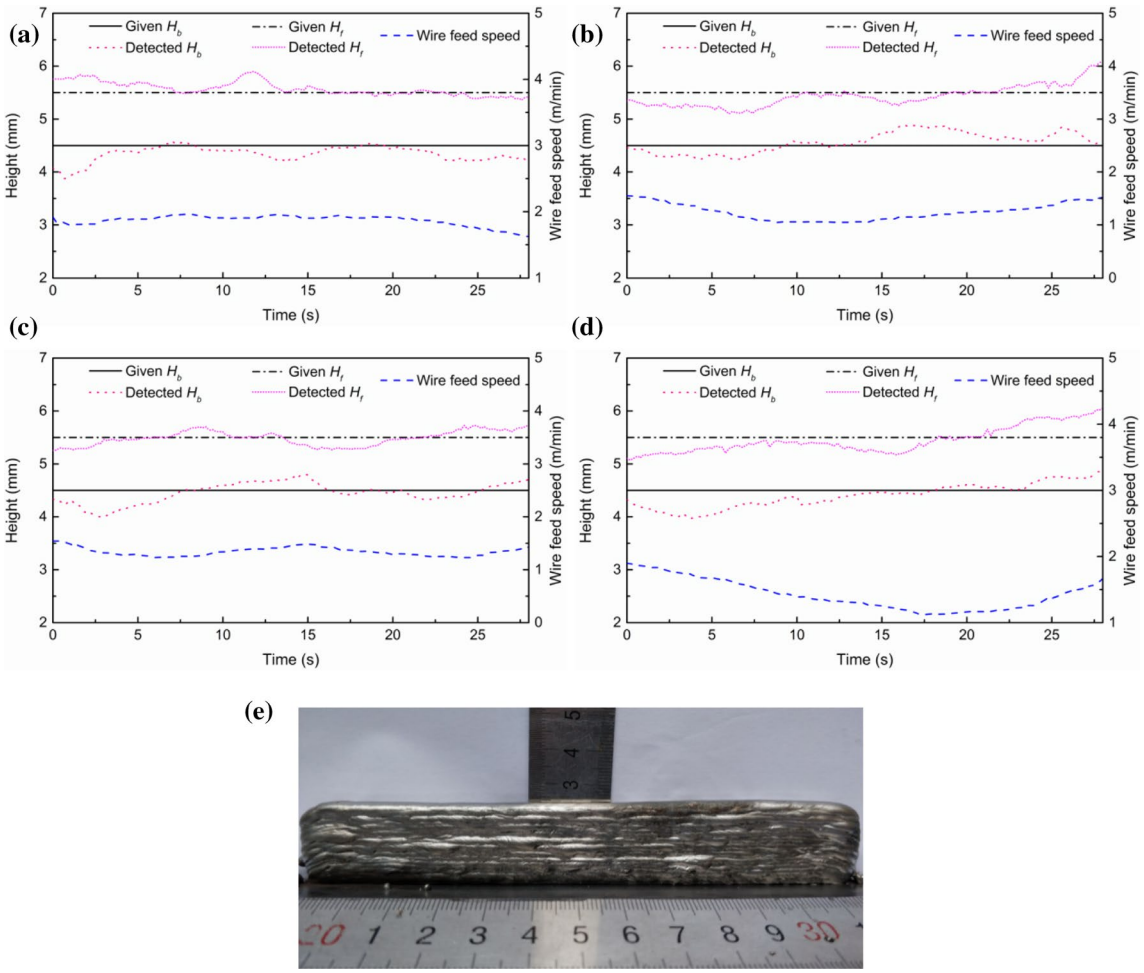

Fig. 7 Closed-loop control experiment based on the visual detection of previous and current heights. **a** Detected H_b, H_f, and wire feed speed in 9th layer. **b** Detected H_b, H_f, and wire feed speed in 13th layer. **c** Detected H_b, H_f, and wire feed speed in 19th layer. **d** Detected H_b, H_f, and wire feed speed in 23th layer. **e** Macroscopic morphology of a 25-layered wall

controller. Increasing the time lag is associated with the increase of the distance between curve peaks of detected *Hb*. By adding the previous height information into the detected current height, it is beneficial to increase the response speed of the feedback controller. Particularly, if the detection point on the top surface of the previous layer presents a hump or a pit, the closed-loop controller can adjust the wire feed speed in advance when the GTA torch is located at the detection point.

Conclusions

With the aim to improve the process stability and forming accuracy in GTA AM, a vision sensing system including previous and current layer detection is designed and a closed-loop controller is proposed to adjust the wire feed speed to compensate for deviations in deposition height. To avoid disturbances and precisely pick up feature points in the image, image processing techniques consisting of window creation, removing noise, edge detection, threshold segmentation, and Hough transformation are applied for features tracking. Furthermore, the user interface is developed to offer information interchange between an operator and the detection as well as control system. Experiments are performed to investigate the effectiveness of the proposed sensing and control system. The results show that the process stability can be improved and the deposition height is approximately consistent with the given height by employing the closed-loop using the current height detection. However, the fluctuation degree of the deposition height increases along with the number of layers. Hence, the previous height deviation, representing the accumulated deviation of previously deposited layers, is introduced into the current height deviation, and the closed-loop control based on this idea improves the deposition height flatness. A shortcoming of

this work is that the bead width is not considered. To address this, simultaneous control of deposition width and height is a subject of future research. Moreover, the developed visual sensing method is not suitable for multi-layer multi-pass parts deposited in WAAM.

Acknowledgements This work was funded by National Natural Science Foundation of China, Nos. 51975491 and 61573293, Sichuan Science and Technology Program, Nos. 2020JDRC0059, 2020YFG0197, and 2019YFG0354, and the Fundamental Research Funds for the Central Universities, No. 2682019CX12.

References

Baxes, G. A. (1994). *Digital image processing: Principles and applications*. New York: Wiley.

Bonaccorso, F., Cantelli, L., & Muscato, G. (2011). An arc welding robot control for a shaped metal deposition plant: Modular software interface and sensors. *IEEE Transactions on Industrial Electronics, 58,* 3126–3132.

Cadiou, S., Courtois, M., Carin, M., Berckmans, W., & Le Masson, P. (2020). Heat transfer, fluid flow and electromagnetic model of droplets generation and melt pool behaviour for wire arc additive manufacturing. *International Journal of Heat and Mass Transfer, 148,* 119102.

Chabot, A., Rauch, M., & Hascoet, J. Y. (2019). Towards a multi-sensor monitoring methodology for AM metallic processes. *Welding in the World, 63*(3), 759–769.

Comas, T. F., Diao, C. L., Ding, J. L., Williams, S., & Zhao, Y. F. (2017). A passive imaging system for geometry measurement for the plasma arc welding process. *IEEE Transactions on Industrial Electronics, 64,* 7201–7209.

Demir, A. G. (2018). Micro laser metal wire deposition for additive manufacturing of thin-walled structures. *Optics and Lasers in Engineering, 100,* 9–17.

Ding, Y. Y., Huang, W., & Kovacevic, R. (2016). An on-line shape-matching weld seam tracking system. *Robotics and Computer-Integrated Manufacturing, 42,* 103–112.

Doumanidis, C., & Kwak, Y. M. (2002). Multivariable adaptive control of the bead profile geometry in gas metal arc welding with thermal scanning. *International Journal of Pressure Vessels and Piping, 79,* 251–262.

Han, Q. L., Li, D. Y., Sun, H. J., & Zhang, G. J. (2019). Forming characteristics of additive manufacturing process by twin electrode gas tungsten arc. *International Journal of Advanced Manufacturing Technology, 104,* 4517–4526.

Ho, A., Zhao, H., Fellowes, J. W., Martina, F., Davis, A. E., & Prangnell, P. B. (2019). On the origin of microstructural banding in Ti-6Al4V wire-arc based high deposition rate additive manufacturing. *Acta Materialia, 166,* 306–323.

Li, Y. J., Yu, S. F., Chen, Y., Yu, R. Z., & Shi, Y. S. (2020). Wire and arc additive manufacturing of aluminum alloy lattice structure. *Journal of Manufacturing Processes, 50,* 510–519.

Marinelli, G., Martina, F., Ganguly, S., & Williams, S. (2019). Development of wire plus arc additive manufacture for the production of large-scale unalloyed tungsten components. *International Journal of Refractory Metals & Hard Materials, 82,* 329–335.

Marr, D., & Hildreth, E. (1980). Theory of edge detection. *Proceedings of the Royal Society of London Series B, 207,* 187–217.

Otsu, N. (1979). A threshold selection method from gray-level histograms. *IEEE Transactions on Systems, Man, and Cybernetics, 9,* 62–66.

Panchagnula, J. S., & Simhambhatla, S. (2018). Manufacture of complex thin-walled metallic objects using weld-deposition based additive manufacturing. *Robotics and Computer-Integrated Manufacturing, 49,* 194–203.

Radel, S., Diourte, A., Soulie, F., Company, O., & Bordreuil, C. (2019). Skeleton arc additive manufacturing with closed loop control. *Additive Manufacturing., 26,* 106–116.

Van, D., Dinda, G. P., Park, J., Mazumder, J., & Lee, S. H. (2020). Enhancing hardness of Inconel 718 deposits using the aging effects of cold metal transfer-based additive manufacturing. *Materials Science and Engineering A, 776,* 139005.

Venturini, G., Montevecchi, F., Bandini, F., Scippa, A., & Campatelli, G. (2018). Feature based three axes computer aided manufacturing software for wire arc additive manufacturing dedicated to thin walled components. *Additive Manufacturing, 22,* 643–657.

Wang, H., & Kovacevic, R. (2001). Rapid prototyping based on variable polarity gas tungsten arc welding for a 5356 aluminium alloy. *Proceedings of the Institution of Mechanical Engineers, Part B: Journal of Engineering Manufacture, 215,* 1519–1527.

Williams, S. W., Martina, F., Addison, A. C., Ding, J., Pardal, G., & Colegrove, P. (2016). Wire + arc additive manufacturing. *Materials Science and Technology, 32,* 641–647.

Wu, B. T., Pan, Z. X., Ding, D. H., Cuiuri, D., Li, H. J., & Fei, Z. Y. (2018). The effects of forced interpass cooling on the material properties of wire arc additively manufactured Ti6Al4V alloy. *Journal of Materials Processing Technology, 258,* 97–105.

Xiong, J., Li, Y. J., Li, R., & Yin, Z. Q. (2018). Influences of process parameters on surface roughness of multi-layer single-pass thin-walled parts in GMAW-based additive manufacturing. *Journal of Materials Processing Technology, 252,* 128–136.

Xiong, J., Yin, Z. Q., & Zhang, W. H. (2016). Closed-loop control of variable layer width for thin-walled parts in wire and arc additive manufacturing. *Journal of Materials Processing Technology, 233,* 100–106.

Xiong, J., & Zhang, G. J. (2014). Adaptive control of deposited height in GMAW-based layer additive manufacturing. *Journal of Materials Processing Technology, 214,* 962–968.

Xiong, J., Zhang, G. J., Hu, J. W., & Wu, L. (2014). Bead geometry prediction for robotic GMAW-based rapid manufacturing through a neural network and a second-order regression analysis. *Journal of Intelligent Manufacturing, 25,* 157–163.

Yang, D. Q., Wang, G., & Zhang, G. J. (2017). Thermal analysis for single-pass multi-layer GMAW based additive manufacturing using infrared thermography. *Journal of Materials Processing Technology, 244,* 215–224.

Yi, H. J., Kim, J. W., Kim, Y. L., & Shin, S. (2020). Effects of cooling rate on the microstructure and tensile properties of wire-arc additive manufactured Ti-6Al-4V alloy. *Metals and Materials International*. https://doi.org/10.1007/s12540-019-00563-1.

Zhang, S., Zhang, Y. Z., Gao, M., Wang, F. D., Li, Q., & Zeng, X. Y. (2019). Effects of milling thickness on wire deposition accuracy of hybrid additive/subtractive manufacturing. *Science and Technology of Welding and Joining, 24,* 375–381.